Journal of Manufacturing Processes 60 (2020) 447–456

Contents lists available at ScienceDirect

Journal of Manufacturing Processes

journal homepage: www.elsevier.com/locate/manpro

Plasma-based isotropic etching polishing of synthetic quartz

Rulin Li [a], Yongjie Zhang [a], Yi Zhang [a], Wang Liu [a], Yaguo Li [b,*], Hui Deng [a,*]

[a] Department of Mechanical and Energy Engineering, Southern University of Science and Technology, No. 1088, Xueyuan Road, Shenzhen, Guangdong 518055, China
[b] Fine Optical Engineering Research Centre, Chengdu, Sichuan 610041, China

ARTICLE INFO

Keywords:
Polishing
Synthetic quartz
Isotropic etching polishing
Inductively coupled plasma
Roughness

ABSTRACT

To efficiently eliminate the surface defects and subsurface damage layer of synthetic quartz introduced by grinding, a plasma-based isotropic etching polishing (plasma-IEP) technique is proposed in this study. The smoothing of synthetic quartz by plasma-IEP is attributed to the formation, overlapping and merging of numerous and ultra-smooth etch pits formed by isotropic etching of SiO_2 using inductively coupled plasma. Plasma diagnostics have revealed the existence of large amounts of etching radicals. The input radio frequency power and CF_4 flow rate have been proved to be the two determinant factors of the material removal rate (MRR) of plasma-IEP. Under the optimized conditions, a maximum MRR of 5.62 μm/min of a 2-inch wafer has been achieved which is much higher than that of the conventional CMP process. After plasma-IEP for 30 min, the *Sa* roughness of the ground synthetic quartz decreases from 270.6 nm to 17.4 nm and the inner surface of the isotropic etch pits is smooth at the atomic level. The results presented in this paper demonstrate that plasma-IEP is a promising approach for the highly efficient and damage-free semi-finishing of synthetic quartz.

Introduction

Compared with fused silica, synthetic quartz has a higher purity up to 99.99999%, and it performs high transparency in the deep ultraviolet region and possesses excellent optical uniformity and good durability under laser irradiation. Thus, synthetic quartz has been widely used in semiconductor and optical industry [1,2]. The performance of synthetic quartz components is strongly dependent on the surface quality. It has been reported that synthetic quartz components are easily damaged under high-energy laser irradiation caused by the defects like surface scratches, cracks, and subsurface damages introduced by mechanical processes [3,4]. Thus, it is indispensable to obtain a damage-free synthetic quartz surface, in order to maintain the performance and reliability of synthetic quartz components.

For the fabrication of synthetic quartz components, some volumetric removal machining processes such as cutting and grinding are generally performed with controllable form accuracy [5]. For cutting or grinding of synthetic quartz, a rough surface with micron meter level surface roughness can be achieved efficiently under the action of a diamond tool or a grinding wheel. However, the surface and subsurface damages are inevitably introduced due to the brittle fracture of synthetic quartz [6,7]. As a consequence, a subsequent finishing process to eliminate both the surface and subsurface damages and to improve the surface roughness is essential. In the past decades, various finishing techniques have been developed to obtain synthetic quartz substrates with excellent surface quality [8]. Qiu et al. [9] proposed the chemical mechanical grinding (CMG) technique which combined chemical reaction and mechanical grinding via a special wheel made of cerium oxide and binding agent. In CMG, a more easily removable silicic acid gel film is formed by the chemical reaction between the grinding wheel, the grinding fluid, and the SiO_2 workpiece; The film is subsequently removed by abrasion in the grinding process; By optimizing the grinding pressure, wheel speed, grinding fluid flow, and pH value, the subsurface damaged (SSD) layer can be reduced and a smooth surface with the *Sa* roughness of 0.795 nm has been achieved. To further improve the surface quality, chemical mechanical polishing (CMP) has been widely used as the finishing technique of synthetic quartz. In CMP process, a modified layer with low brittleness is formed based on the chemical reaction between the corrosive chemical slurry and SiO_2, and it is then removed by the abrasives, leading to an ultra-smooth surface with sub-nanometer roughness. In general, the alkaline CeO_2 based slurry is widely used in CMP of synthetic quartz. Due to the low mechanical load of CMP, the subsurface damage layer introduced by previous mechanical process can be eliminated, but the material removal rate (MRR) is relatively low. Meanwhile, CeO_2 is a not only expensive but also toxic chemical, which would severely pollute the environment [10,11]. To solve the above

* Corresponding authors.
E-mail addresses: yargolee@163.com (Y. Li), dengh@sustech.edu.cn (H. Deng).

https://doi.org/10.1016/j.jmapro.2020.10.075
Received 15 July 2020; Received in revised form 10 September 2020; Accepted 27 October 2020

problems, SiO_2 based slurry was developed. It has been demonstrated that a *R*q roughness below 0.2 nm and an MRR of 1 μm/h can be achieved using alkaline SiO_2 slurry. As for acid SiO_2 slurry, the MRR can be improved to 10.9 μm/h, while the *R*q roughness remains 0.193 nm [5].

To form a thoroughly damage-free synthetic quartz surface, non-contact machining processes are of first priority. Thus, wet or dry etching of synthetic quartz has been studied by many researchers. Wang et al. studied the morphological evolution of the ground quartz surface during HF etching, and found that etching with high concentration HF solution could promote the extension and mutual interleaving of cracks, eliminating the SSD layer of synthetic quartz eventually. The etching rate of concentrated HF is as high as 1.14 μm/min and the surface form accuracy of workpiece can be basically kept unchanged after etching [12,13]. Additionally, dry etching using atmospheric pressure plasma has also been developed for damage-free processing of synthetic quartz. Takino et al. proposed a capacity coupled plasma (CCP) based chemical vaporization machining (CVM) technique to achieve the correction of form errors of steep spheres. SF_6 was used as the reactive gas for the generation of fluorine radicals via dissociation while the workpiece was exposed to plasma for etching. The movement of the workpiece was monitored by mounting on a three-axis motion control platform, while the dwelling time was calculated by a de-convolution algorithm. As a result, the substrate with highly accurate smooth surface with the desired rms shape accuracy of 3 nm was successfully obtained [14]. To reduce the process cost of helium-based CCP system, plasma CVM using argon-ethanol mixture gas as the carrier gas was proposed for correcting the thickness deviation of a quartz crystal wafer [15]. Besides, inductively coupled plasma (ICP) processing technologies are also well-developed for silicon-based materials. Jourdain et al. devised a Helios 1200 machine to figure meter sized optical surface and achieved form accuracy correction better than 20 nm rms by Reactive atom plasma (RAP) technology utilizing ICP etching. [16]. Castelli et al. also obtained a fused silica substrate with residual errors down to 16 nm rms (λ/40 rms) with the assistance of RAP technology [17]. Xin et al. proposed an atmospheric pressure plasma process based on ICP and studied the surface morphology evolution of ground fused silica [18]. Yu et al. studied aerodynamic properties of ICP jet based on computational fluid dynamics to support the optimization of ICP torch design [19]. In order to maintain a stable discharge of plasma for long period, a robust plasma delivery system (PDS) was developed for manufacturing of large optics. Using the optimum parameters of the PDS, a 70 mm × 200 mm fused silica sample was processed to achieve a flatness of 10 nm in RMS within 20 min [20].

Although it has been demonstrated that wet and dry etching is capable to efficiently remove the SSD layer on synthetic quartz substrates, it is challenging to smooth the surface via chemical etching. Yi et al. proposed an isotropic etching polishing (IEP) technique as a generic approach for the damage-free and ultrasmooth polishing of metals. In IEP processing, electrochemical etching occurred at the breakdown sites on the metal surface, while the isotropic etching of the metal surface was realized by adjusting the concentration ratio of the electrolyte and the etching temperature to form ultra-smooth hemispherical holes. With the increase of the etching duration, the hemispherical etching holes became larger and began to overlap. Consequently, the entire rough surface was completely replaced by the smooth inner surface of the newly formed hemispherical etched holes. For the IEP of titanium alloy, a smooth surface with the *S*a roughness of 1.2 nm was obtained with a maximum polishing rate of 15 μm/min [21]. According to the mechanism of IEP, the key to realize the smoothing effect of IEP is isotropic etching, either by electrochemical etching or other etching approaches. Zhang et al. successfully applied IEP in SiC polishing by molten KOH etching [22]. Ultrafast polishing of a sliced SiC substrate was achieved with the surface roughness *S*a reduced from 246.5 nm to 16.06 nm within 2 min at 800 °C and the SSD layer has been completely removed.

Up to now, plasma etching has been widely used for machining of silicon-based materials. However, the mechanism of surface smoothing via plasma isotropic etching has never been introduced. In this study, a plasma-based IEP process is proposed to efficiently achieve a damage-free and smooth surface of synthetic quartz. In plasma-IEP of synthetic quartz, the surface is polished through isotropic etching induced by atmospheric pressure ICP. Plasma diagnostics was carried out to investigate the radical properties in plasma. The MRR of plasma-IEP has been evaluated to reveal the determinant parameters of the polishing efficiency. The surface morphology and roughness evolution during plasma etching has been studied to demonstrate the polishing mechanism of plasma-IEP.

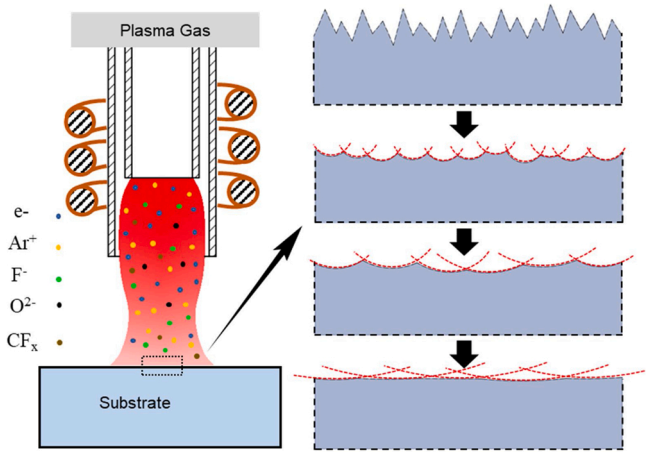

Fig. 1. Schematic diagram of plasma-IEP of synthetic quartz.

Principle of plasma-IEP

The plasma-IEP process of synthetic quartz via ICP is based on the chemical reaction between radicals in CF_4 plasma and SiO_2. Atmospheric pressure ICP has been generally admitted to possess both higher temperatures (5000-7000 K) and higher radical density (10^{13}–10^{17} cm^{-3}) [23]. That is the reason why the atmospheric ICP is considered to be an ideal approach for highly efficient dry etching. A high density of fluorine radicals is generated by electron impact dissociation of CF_4 in ICP. The fluorine radicals with strong chemical reactivity are adsorbed by the synthetic quartz substrate and then the etching reaction happens [18]. The etching reaction can be expressed as Eq. (1):

$$SiO_2 + CF_4 \rightarrow SiF_4\uparrow + CO_2\uparrow \quad (1)$$

Obviously, plasma-IEP is a gaseous etching process without any mechanical stress, which makes it an ideal method to eliminate the surface defects and subsurface damage layer of synthetic quartz. Fig. 1 illustrates the smoothing mechanism of plasma-IEP. At the beginning of the polishing process, many etching sites are randomly formed on the substrate. Isotropic etching reaction occurs at these etching sites, resulting in the formation of hemispherical etch pits with the smooth inner surfaces. With the increasing of etching duration, the diameter of the etch pits becomes larger, which makes the adjacent pits begin to overlap and gradually merge into the bigger etch pits. The surface roughness of synthetic quartz decreases gradually due to the decreasing height difference between the boundary and the bottom of the overlapped pits. Ultimately, the original rough surface of synthetic quartz is replaced by the smooth inner surfaces of the overlapped hemispherical etch pits. In the plasma-IEP process, the final surface quality is determined by the diameter and density of the etch pits. The smoothing mechanism of plasma-IEP is very similar to that of electrochemistry-IEP [21]. Theoretically, the larger the diameter of the etch pits, the lower the achievable surface roughness of synthetic quartz.

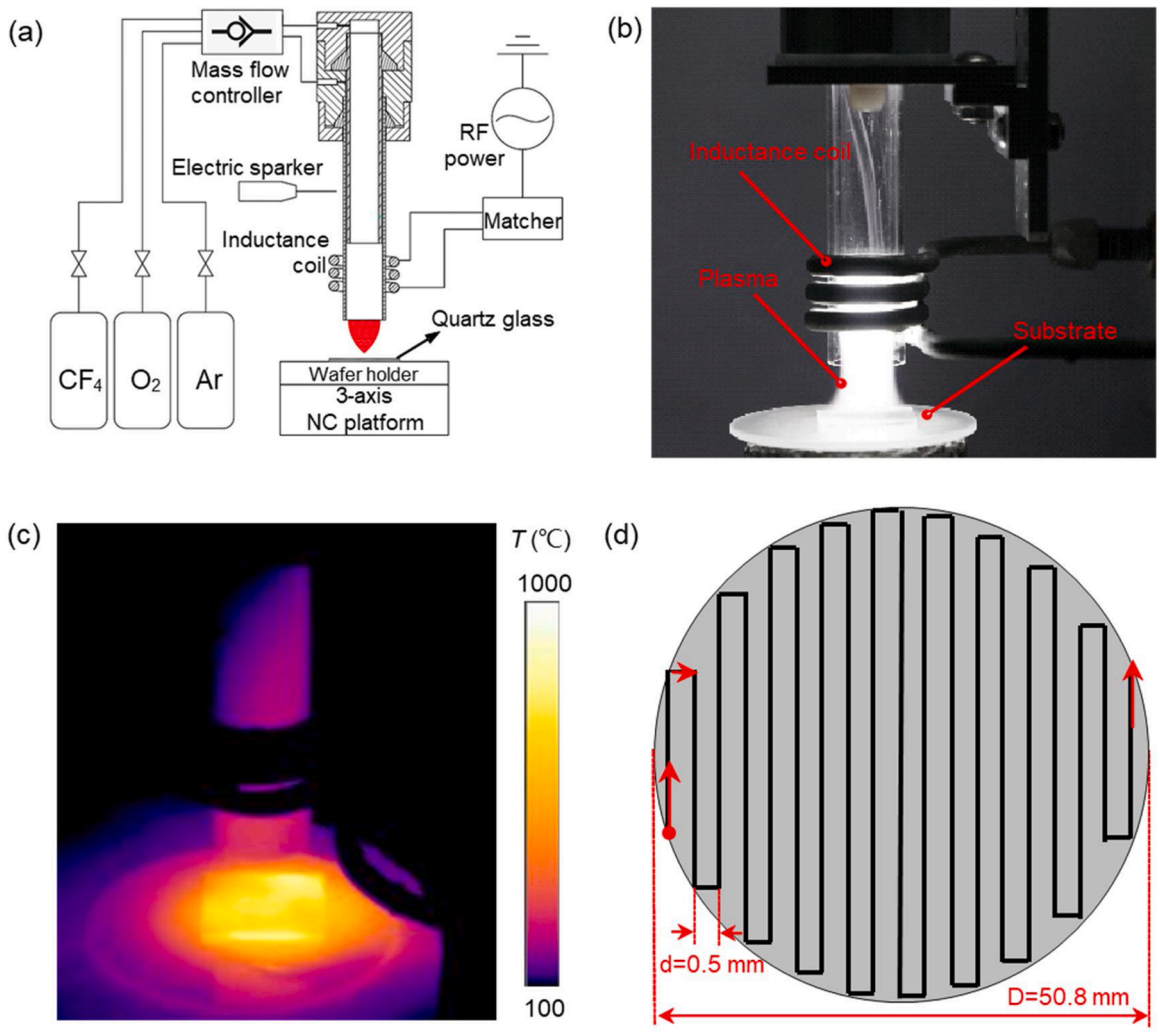

Fig. 2. (a) Schematic diagram of plasma-ICP setup. (b) Optical photo of ICP torch. (c) Thermal image of the substrate during plasma-IEP. (d) The scanning routine of ICP torch.

Experimental details

Materials

Commercial synthetic quartz wafers which were originally process by CMP with a diameter of 2 inches and a thickness of 2 mm were used to measure the MRR of plasma-IEP. Synthetic quartz substrates which were originally process by rough grinding with the size of 20 mm × 20 mm × 1 mm were used to study the etching characteristics and smoothing mechanism of plasma-IEP. Before the experiments, all samples were ultrasonically cleaned by ultrapure water and high purity alcohol (99.5%) in sequence, following by being dried with nitrogen (99.999%) gas blowing.

Plasma-IEP setup

Fig. 2(a) shows the schematic diagram of the ICP setup used in plasma-IEP of synthetic quartz. The setup consists of an RF power (40.68 MHz), an impedance matcher, a copper inductance coil, a quartz torch, a water-cooling circulation system, and so forth. The quartz torch, which was fixed in the center of the inductive coil, was composed of two coaxial quartz tubes; the ignition gas (Ar) and the reaction gases (CF_4 and O_2) were supplied through the inner tube, and the role of oxygen was to avoid the formation of fluoropolymer and facilitate the dissociation of CF_4 [24,25]; the outer tube was supplied with the cooling gas (Ar) to prevent the tube from being heated to melt and to stabilize the plasma torch. Under the cooperation of the above components and parts, plasma was generated in the quartz torch, as shown in Fig. 2(b). In the IEP process, the sample was placed on a wafer holder made of high temperature resistant aluminum oxide ceramics. And the movement of the wafer holder was controlled by a three-axis numerical control (NC) platform. According to the thermal image of the quartz sample shown in Fig. 2c, the average surface temperature of the substrate was 738.9 °C when the RF power was set at 600 W. Fig. 2(d) shows the scanning routine of plasma-IEP of a 2-inch synthetic quartz wafer.

Characterizations and measurements

In this study, the MRR of synthetic quartz by plasma-IEP was evaluated using a precision balance (METTLER CC-3372-02). The composition of radicals in ICP was determined by an optical emission spectrometer (OES, Ocean optics USB4000) with the wavelength resolution of 0.2 nm. To evaluate the temperature of the synthetic quartz samples during plasma etching, a thermal imaging camera (FLIR T660) was used. The morphological characterization was conducted using a laser scanning confocal microscopy (LSCM, KEYENCE VK-X1000). The surface roughness was measured by a scanning white light interferometer (SWLI, Taylor Hobson M112-4449-02 CCI HD) and an atomic force microscope (AFM, BRUKER Dimension edge, tapping mode).

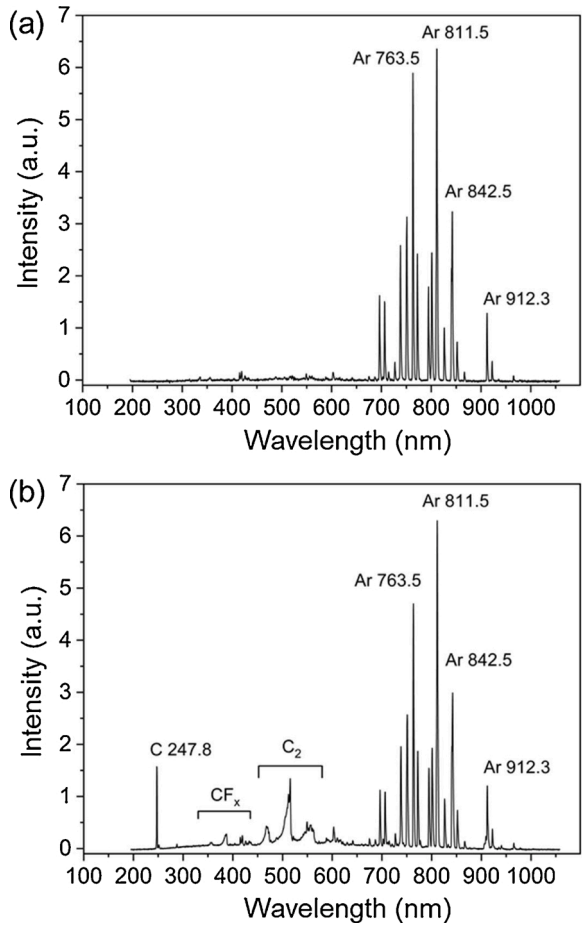

Fig. 3. OES spectra of the ICP torch. (a) Plasma with pure Ar. (b) Plasma with a mixture of Ar, CF_4, and O_2.

Results and discussion

Plasma diagnostics by OES

To investigate the radical characteristics in the plasma, OES has been employed and the typical OES spectra of the ICP torch at 600 W are shown in Fig. 3. When only the ignition gas (Ar, 1.0 slm) was supplied, some strong argon peaks (751.5, 763.5, 811.5 842.5, 912.3 nm), which are corresponding to the deexcitation of argon atoms, can be seen clearly as shown in Fig. 3(a) [26,27]. After adding CF_4 (60 sccm) and O_2 (10 sccm) as the reaction gases, the peaks corresponding to CF_x (280-400 nm), C peak (247.8 nm), and C_2 radicals (Swan bands) are remarkable, as shown in Fig. 3(b) [28–30]. Due to the small difference between the peak positions of the fluorine peaks and argon peaks as well as the limited wavelength resolution of the spectrometer, the peaks of fluorine radicals could not be identified. However, the existing peaks of CF_x and C_2 can prove the dissociation process of CF_4, and this process would inevitably generate the atomic fluorine, which is the main etching reactant in plasma-IEP of synthetic quartz [31]. Besides, some weak peaks corresponding to nitrogen (316, 337, 357, 380 nm) can also be observed due to the participation of the ambient air during plasma discharge [32,33].

MRR of Plasma-IEP

In the plasma-IEP process, the material removal of synthetic quartz is based on the chemical etching between CF_4 plasma and SiO_2. To prove the high efficiency of plasma-IEP, the MRR of 2-inch synthetic quartz wafers under different conditions were investigated. And the MRR can be calculated by Eq. (2) [34]:

$$MRR = \frac{\Delta m}{\rho \pi R^2 t} \tag{2}$$

where Δm represents the weight change of the wafer before and after plasma-IEP; ρ is the density of synthetic quartz, which is 2.2 g·cm^{-3}; R is the radius of the synthetic quartz wafer, which is 25.4 mm in this study; t is the processing time. Table 1 shows the processing parameters of Plasma-IEP in the scanning mode. Based on the scanning routine shown in Fig. 2(c), the whole surface of the wafer can be polished uniformly by plasma. In this study, MRR is mainly affected by the reaction temperature and the concentration of fluorine radicals. The former is controlled by the RF input power, and the latter depends on the CF_4 flow rate. Therefore, we mainly focus on the MRR of synthetic quartz etched by plasma under different RF power and CF_4 flow rates.

Fig. 4(a) shows the MRR with the RF power ranging from 300 W to 900 W, where the flow rate of CF_4 is constant at 30 sccm. It can be seen

Table 1
Processing parameters of plasma-IEP in scanning mode.

Parameter	Value
Ignition gas flow rate (Ar)	1.5 slm
Cooling gas flow rate (Ar)	13 slm
CF_4 flow rate	0-80 sccm
Processing distance	15 mm (torch-to-wafer)
RF power	300-900 W
Scanning speed	150 mm/min
Time	12.5 min

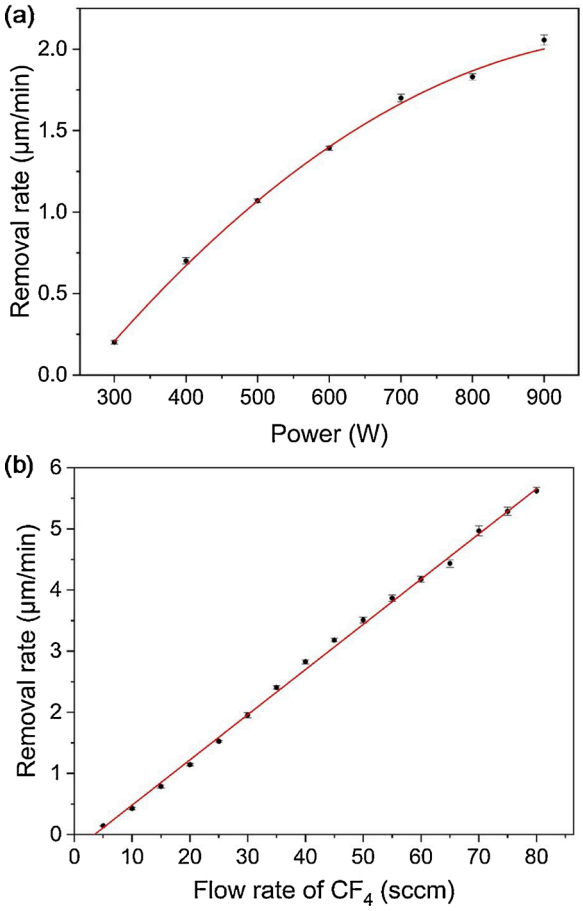

Fig. 4. Variation of MRR of plasma-IEP with different RF power and flow rate of CF_4. (a) MRR versus RF power. (b) MRR versus CF_4 flow rate.

Table 2
Processing parameters of plasma-IEP in static mode.

Parameter	Value
Ignition gas flow rate (Ar)	1.0 slm
Cooling gas flow rate (Ar)	18 slm
CF_4 flow rate	10-80 sccm
O_2 flow rate	10 sccm
Processing distance	12 mm (torch-to-wafer)
RF power	300-800 W
Time	1-30 min

that the MRR significantly increases with the increase of RF power. As previously described, the increase in RF power directly leads to an increase in the surface temperature of the wafer. Thus, it can be concluded that the MRR is positively correlated with the reaction temperature. And the increasing rate of MRR decreases with the increase of RF power which is considered owing to the near saturated etching conditions. Fig. 4(b) shows the MRR with the CF_4 flow rate ranging from 5 to 80 sccm, where the RF power is kept constant at 800 W. Since the plasma torch was exceedingly unstable and the quartz tube became severely corroded by the high concentration of fluorine radicals when the CF_4 flow rate exceeded 80 sccm, therefore the experiment with the CF_4 flow rate over 80 sccm was not conducted in this study. It is clear that the MRR increases almost linearly with the increase of the CF_4 flow rate, which is attributed to the increase of the fluorine radical concentration in plasma. Noticeably, the above tendency is in correspondence with Arrhenius equation: [35,36]

$$MRR(T) = n_F A exp(\frac{-E_a}{RT}) \quad (3)$$

where A is the pre-exponential factor, which is a constant for the specific reaction; n_F is the concentration of fluorine radicals; E_a is the reaction activation energy; R is the universal gas constant; T is the absolute temperature of the sample surface. Based on the above results, the maximum MRR of synthetic quartz by plasma-IEP can reach 5.62 μm/min, which is far greater than that of conventional CMP process. Owing to the high efficiency of plasma-IEP, the damage layer of synthetic quartz caused by mechanical processing can be quickly removed. Thus, plasma-IEP can be considered as a very promising technology for highly efficient processing of synthetic quartz.

Isotropic etching of synthetic quartz by plasma-IEP

To investigate the isotropic etching characteristics of synthetic quartz in plasma-IEP, static etching with substrate or plasma scanning was conducted. This was because the new etch pits were inevitably formed during scanning plasma etching and it would become difficult to analyze the anisotropy, density and growth of the etch pits. Due to the limited length of plasma torch and small etching area in static mode, the processing distance and Ar flow rates were changed to obtain a larger smoothed area by plasma-IEP. The parameters for static plasma etching are shown in Table 2. Fig. 5 shows the processing results under different etching durations with the constant RF power (500 W) and CF_4 flow rate (60 sccm). As shown in Fig. 5(a), the original as-ground synthetic quartz surface was covered with surface defects. After processed by plasma-IEP for 10 s (Fig. 5(b)), the subsurface damages such as cracks were exposed and then expanded greatly as processing time extended to 20 s (Fig. 5(c)). As shown in Fig. 5(d), the exposed subsurface damage was nearly replaced by etch pits which distributed on the entire surface. When the processing duration was extended to 1 min, as shown in Fig. 5(e), the

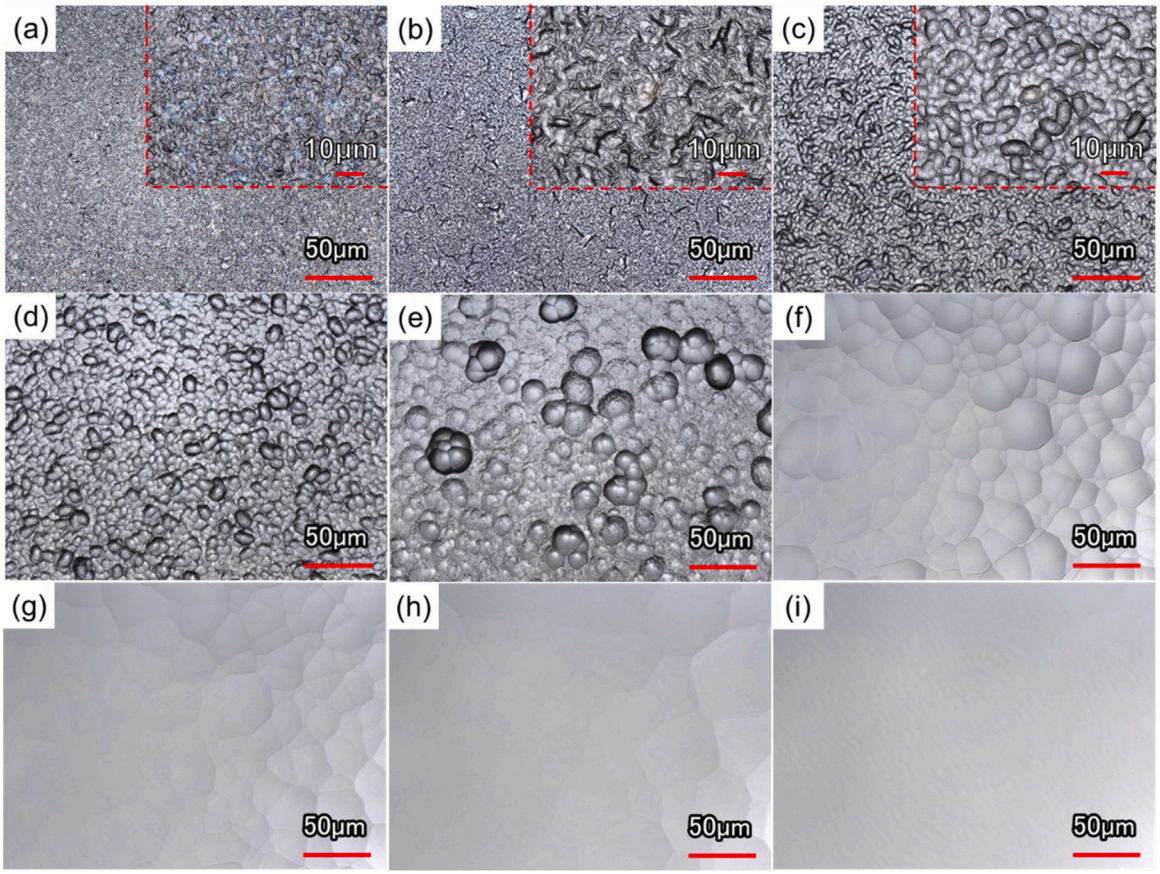

Fig. 5. LSCM images of the etched surfaces under different etching durations with the constant RF power (500 W) and CF_4 flow rate (60 sccm). (a) Original surface, (b) 10 s, (c) 20 s, (d) 40 s, (e) 1 min, (f) 5 min, (g) 10 min, (h) 20 min, and (i) 30 min.

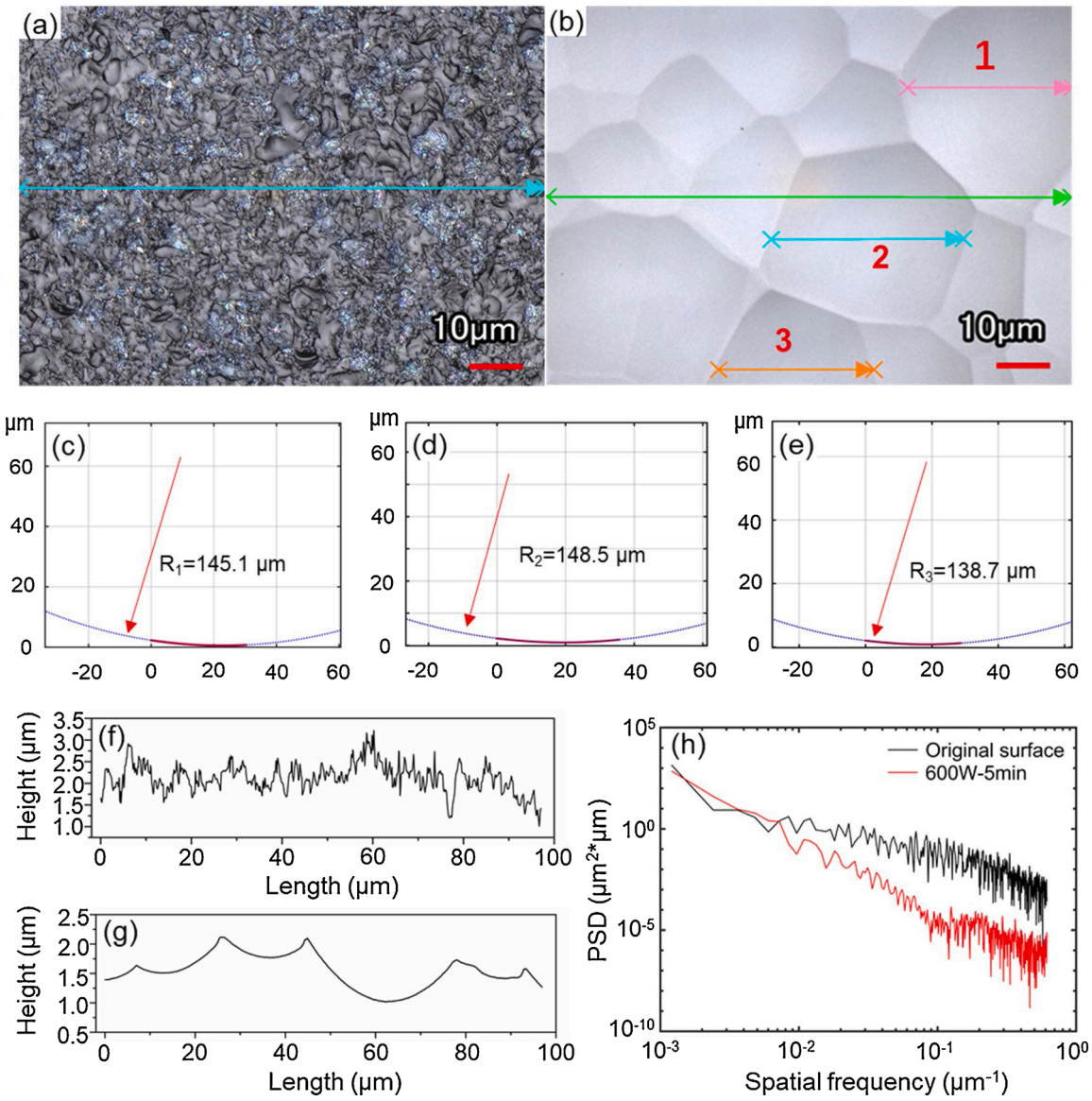

Fig. 6. (a) Original surface of synthetic quartz. (b) ICP etched surface of synthetic quartz (500 W, 5 min, 60 sccm CF_4). (c-e) MATLAB fitting results of three etch pits profiles. (f) Cross-section profile of the original surface. (g) Cross-section profile of the processed surface. (h) PSD curves of the original and plasma etched surfaces.

diameter of the etch pits enlarged as the etching reaction continued and the subsurface damage layer was completely removed, then the adjacent etch pits became overlapped and merged due to the dramatically enlarged pits diameter with increasing of etching duration to 5 min. For the etching results under the longer durations as shown in Fig. 5(d-f), the diameter of the etch pits continued to increase while its density decreased remarkably. The original rough sample surface was gradually replaced by the inner surface of the overlapped etch pits. In Fig. 5(f), the boundaries of the pits were hardly visible, and the synthetic quartz surface became extremely smooth.

As shown in Fig. 6, the profiles of some etch pits were measured by LSCM and it has been verified that the etching process of synthetic quartz via atmospheric ICP was isotropic. Compared with the original surface of synthetic quartz shown in Fig. 6(a), the processed surface is composed of many overlapped etch pits as shown in Fig. 6(b). As shown in Fig. 6(c-e), the red lines are the measured profiles, and the blue lines are the fitting results by Matlab. It has been revealed that all the profiles can be fitted with the circles with specific radii, which are 145.1 μm, 148.5 μm, and 138.7 μm, respectively. Besides, as shown in Fig. 6(f, g), the surface defects were completely removed and the inner surfaces of the etch pits had become ultra-smooth. Thus, we come to the conclusion that the etching reaction between ICP and synthetic quartz is essentially isotropic etching. Additionally, to study the smoothing effect of synthetic quartz via plasma-IEP, power spectral density (PSD) analysis of the original and etched surfaces of synthetic quartz was conducted using Matlab. As shown in Fig. 5(h), after the etching at 500 W for 5 min, the intensity of the high-frequency band decreases sharply; however, the low-frequency band has barely changed due to the existing large height difference between the boundary and the bottom of the etch pits under the current experimental parameters. The above PSD analysis indicates that plasma-IEP can be applied to achieve a great roughness decrease of synthetic quartz.

In the process of plasma-IEP, the surface morphology of synthetic quartz is mainly determined by the evolution of etch pits, which is affected by the flow rate of CF_4 and RF power. Therefore, we further investigated the etching effects under different CF_4 flow rates and RF power. Fig. 7 shows the etched surfaces of synthetic quartz under the conditions of 500 W and 5 min with the CF_4 flow rates ranging from 10 sccm to 80 sccm. It can be found that the diameter of the etch pits increases while its density decreases, with the increase of the CF_4 flow

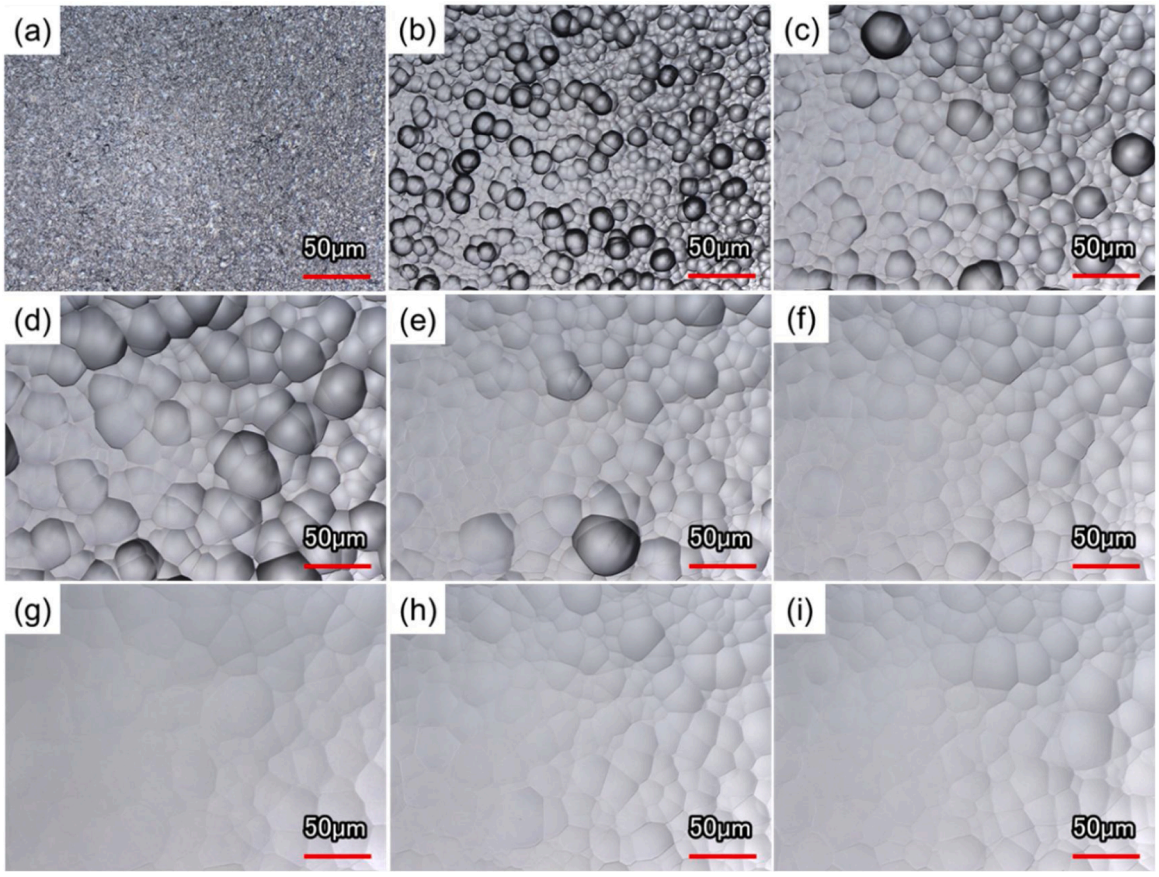

Fig. 7. Evolution of the surface morphology of synthetic quartz under different CF_4 flow rates. (a) Original surface, (b) 10 sccm, (c) 20 sccm, (d) 30 sccm, (e) 40 sccm, (f) 50 sccm, (g) 60 sccm, (h) 70 sccm, and (i) 80 sccm.

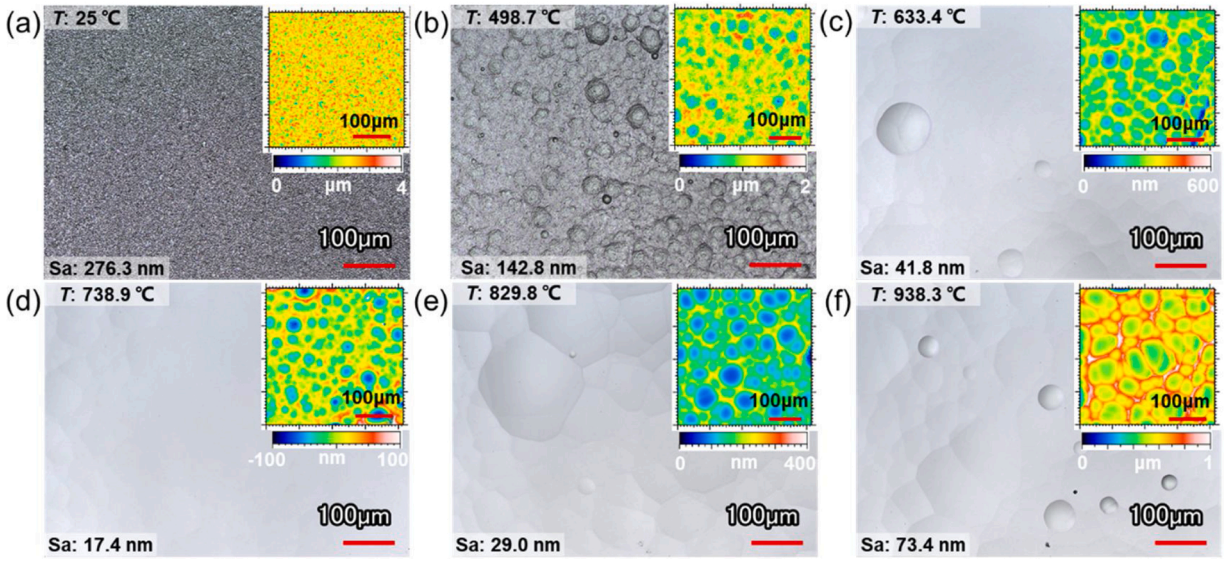

Fig. 8. Evolution of the surface morphology of synthetic quartz under different RF power. (a) Original surface, (b) 400 W, (c) 500 W, (d) 600 W, (e) 700 W, and (f) 800 W. The inserted SWLI images show the corresponding *Sa* roughness.

rate. Thus, it is concluded that the high CF_4 flow rate can speed the etching rate and promote the overlapping and merging process of the etch pits, which is important to realize the smoothing effect of synthetic quartz via plasma-IEP.

Fig. 8 shows the etched surfaces of synthetic quartz at the duration of 30 min with the RF power ranging from 400 W to 800 W. To prevent the quartz tube from being severely etched under high concentration of fluorine radicals, the flow rate of CF_4 is chosen to be 60 sccm. In addition to the surface morphology characterized by a LSCM, we also obtained the accurate *Sa* roughness of the etching samples using a SWLI and the inserted values showed the average temperature measured by thermal image camera, as shown in Fig. 8. Compared with the original surface

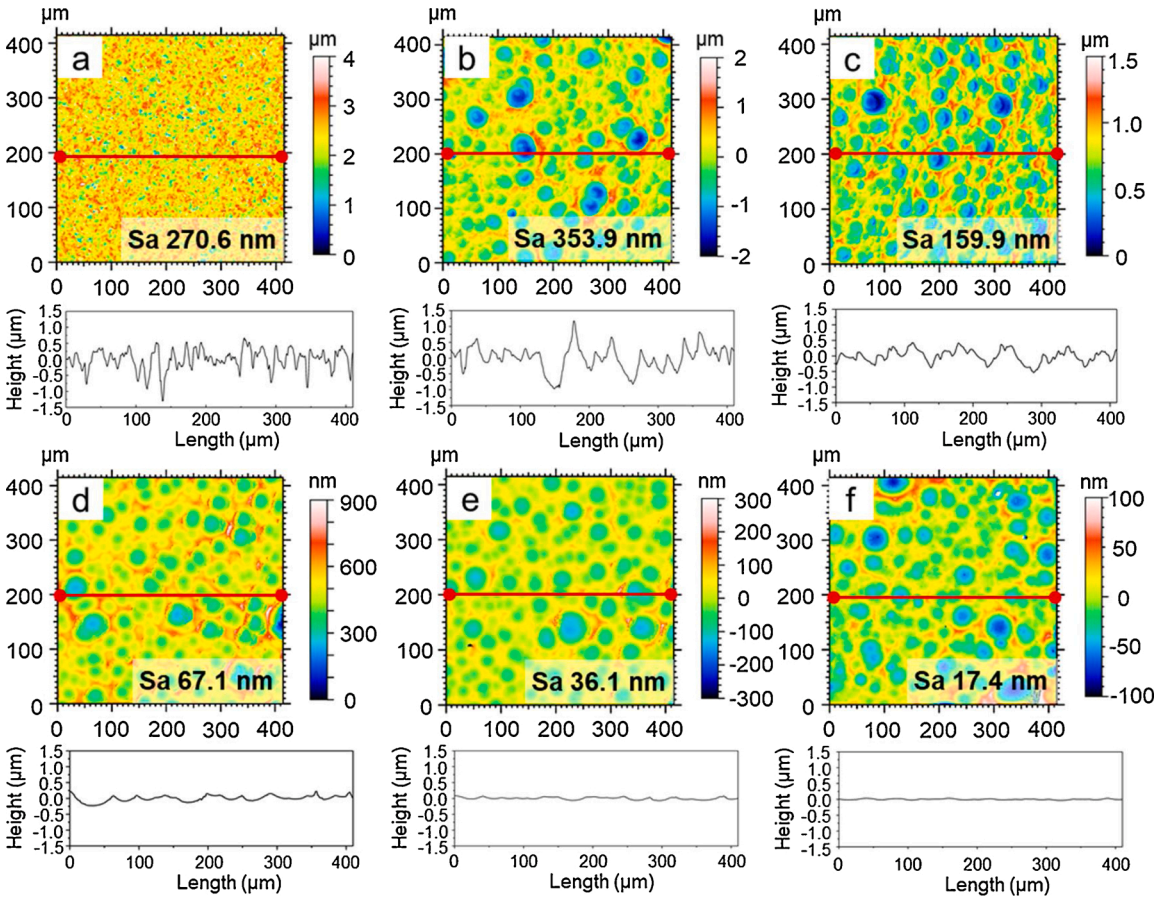

Fig. 9. Evolution of the surface morphology and roughness of synthetic quartz etched at the RF power of 600 W and the CF_4 flow rate of 60 sccm for different etching durations. (a) Original surface, (b) 5 min, (c) 10 min, (d) 15 min, (e) 20 min, and (f) 30 min. The images below show the corresponding cross-section profiles of the samples.

shown in Fig. 8(a), the defects caused by grinding were completely removed under 400 W and the etched surface was covered with the etch pits of different sizes (Fig. 8(b)). At the low RF power, the etching sites were distributed randomly on the sample surface due to the low reaction temperature of 498.7 ℃. During the constant irradiation of plasma, the initially formed etch pits became larger and larger, while the new etch pits were randomly generated in the previous etch pits. The newly generated pits destroyed the smooth profiles of the overlapped big etch pits, which seriously deteriorated the morphology of the etched surface and limited the reduction of its roughness. According to the inserted SWLI image shown in Fig. 8(b), the *Sa* roughness of the etched surface is 142.8 nm. At 500 W (Fig. 8(c)), the temperature of the sample rose to 633.4 ℃, the etched surface was mainly covered with the large etch pits. The number of newly generated etch pits due to the change of etching sites decreased significantly, and the surface roughness decreased to 41.8 nm. When the RF power increased to 600 W, the reaction temperature was 738.9 ℃. As shown in Fig. 8(d), the large etch pits on the sample surface were overlapped uniformly, and no newly generated etch pits were observed. Under this circumstance, the original etch pits kept being enlarged, and the corresponding surface roughness significantly decreased to 17.4 nm. However, for the etching results at 700 W and 800 W shown in Fig. 8(e) and (f), the new etch pits were generated again based on the original etch pits with the further increased temperature, resulting in the increase of the surface roughness. Consequently, we believe that the reaction temperature of 738.9 ℃ at 600 W is more beneficial to promote the growth and overlapping of the original etch pits and to avoid the formation of new etch pits, so as to achieve better surface processing quality of synthetic quartz via plasma-IEP.

Smooth process of synthetic quartz via plasma-IEP

Based on the above results, we consider that the optimal conditions of plasma-IEP for synthetic quartz should be the RF power of 600 W and the CF_4 flow rate of 60 sccm. Under the optimal conditions, the highly efficient and damage-free smoothing of synthetic quartz can be achieved. Fig. 9 shows the change of surface morphology and roughness of the samples etched at the optimal RF power and CF_4 flow rate for different etching durations. At the beginning of polishing process (Fig. 9 (b)), the small etch pits were formed on the sample surface, only a few of which were overlapped and merged. At this moment, the *Sa* roughness increased from the original 270.6 nm to 353.9 nm. As the duration was extended to 10 min, more etch pits got overlapped and merged for the expanding of their diameters, as shown in Fig. 9(c). The growth and overlapping of the etch pits significantly reduced the height difference of the surface profile and the number of these pits, leading to the decrease of *Sa* roughness to 159.9 nm. For the longer etching duration (Fig. 9(d-f)), the *Sa* roughness continued to decrease with the increasing growth and overlapping of the etch pits. As shown in Fig. 9(f), we achieved the smooth synthetic quartz with the *Sa* roughness of 17.4 nm after 30 min etching. Besides, the corresponding cross-section profiles also verified the smoothing process of synthetic quartz with the increasing etching duration.

After the etching at the RF power of 600 W and the CF_4 flow rate of 60 sccm for 30 min, the *Sa* roughness decreased to the minimum value. When the polishing duration was further extended, the surface *Sa* roughness didn't change too much and the *Sa* was still higher than 15.0 nm. The AFM was used to measure the *Sa* roughness of a square area with the side length of 20 μm, which was selected on the inner surface of

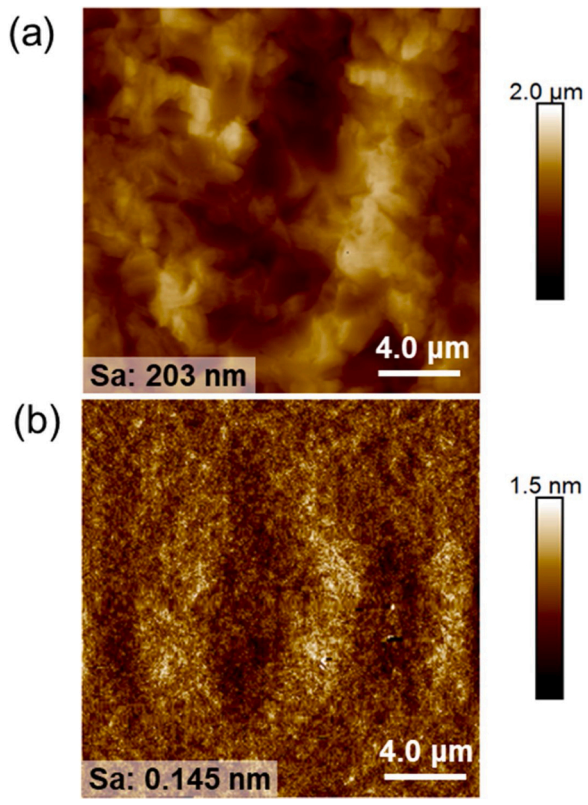

Fig. 10. Comparison of surface morphology and roughness measured by AFM in a micro scale of synthetic quartz. (a) Original surface. (b) Plasma-IEP processed surface.

the etch pits. As shown in Fig. 10, the inner surface of the etch pits is atomically smooth with the *Sa* roughness of 0.145 nm. It is obvious that the existence of the spherical profiles restricted the further decrease of the surface roughness to sub-nm level in a large area. According to the mechanism of IEP, the larger the etch sites are, the lower the surface roughness will be. Thus, how to realize the continuous growth of the etch pits should be further studied.

Though a surface with a *Sa* roughness of 17.4 nm is not smooth enough compared with the surface processed by CMP, plasma-IEP has demonstrated several advantages such as high efficiency, damage-free and sub-nm roughness in micro scales. Thus, it can be concluded that plasma-IEP can be used as a semi-finishing approach for synthetic quartz processed by grinding.

Conclusions

In this paper, plasma-IEP was proposed as a highly efficient and damage-free semi-finishing approach for synthetic quartz. The surface smoothing of synthetic quartz by plasma-IEP is based on the isotropic etching effect. The decrease of the *Sa* roughness is attributed to the overlapping and merging of the etch pits during the growth process, in which the density and diameter of the etch pits collectively determine the smoothing effect. A smoothed surface with *Sa* roughness decreased from 270.6 nm to 17.4 nm after 30 min of plasma-IEP is achieved. For the inner surface of the isotropic etch pits, the *Sa* roughness was only 0.145 nm. The MRR of plasma-IEP is positively related to the RF power and CF_4 flow rate, and the maximum MRR of 5.6 μm/min is obtained. At current stage, this method cannot directly replace the final finishing step, but it can serve as a competitive semi-finishing approach for optical surface of synthetic quartz. And we anticipate that better results can be achieved by a vacuum ICP system with precise temperature control.

Declaration of Competing Interest

The authors declare that they have no known competing financial interests or personal relationships that could have appeared to influence the work reported in this paper.

Acknowledgements

This project is supported by National Natural Science Foundation of China (Grant No. 52035009, 52005243) and the research fund for International Cooperation (GJHZ20180928155412525) from the Science and Technology Innovation Committee of Shenzhen Municipality. The authors also would like to thank the Shenzhen High-level Innovation and Entrepreneurship Fund (No. KQTD20170810110250357) for their financial support. The authors acknowledge the assistance of SUSTech Core Research Facilities.

References

[1] Dekker H, D'Odorico S, Kaufer A, Delabre B, Kotzlowski H. Design, construction, and performance of UVES, the echelle spectrograph for the UT2 Kueyen Telescope at the ESO Paranal Observatory. SPIE; 2000. 4008.
[2] Imai H, Arai K, Hosono H, Abe Y, Arai T, Imagawa H. Dependence of defects induced by excimer laser on intrinsic structural defects in synthetic silica glasses. Phys Rev B 1991;44:4812–8.
[3] Laurence TA, Bude JD, Shen N, Feldman T, Miller PE, Steele WA, Suratwala T. Metallic-like photoluminescence and absorption in fused silica surface flaws. Appl Phys Lett 2009;94:151114.
[4] Li D, Li N, Su X, Liu K, Ji P, Wang B. Characterization of fused silica surface topography in capacitively coupled atmospheric pressure plasma processing. Appl Surf Sci 2019;489:648–57.
[5] Shi XL, Chen G, Xu L, Kang C, Luo G, Luo H, Zhou Y, Dargusch MS, Pan G. Achieving ultralow surface roughness and high material removal rate in fused silica via a novel acid SiO2 slurry and its chemical-mechanical polishing mechanism. Appl Surf Sci 2020;500:144041.
[6] Suratwala T, Wong L, Miller P, Feit MD, Menapace J, Steele R, Davis P, Walmer D. Sub-surface mechanical damage distributions during grinding of fused silica. J Non-Cryst Solids 2006;352:5601–17.
[7] Li Y, Zheng N, Li H, Hou J, Lei X, Chen X, Yuan Z, Guo Z, Wang J, Guo Y, Xu Q. Morphology and distribution of subsurface damage in optical fused silica parts: Bound-abrasive grinding. Appl Surf Sci 2011;257:2066–73.
[8] Zhao L, Cheng J, Chen M, Yuan X, Liao W, Liu Q, Yang H, Wang H. Formation mechanism of a smooth, defect-free surface of fused silica optics using rapid CO2 laser polishing. Int. J. Extrem. Manuf 2019;1:035001.
[9] Qiu ZJ, Zhou LB, Fang FZ, Shina T, Eda HJO. Chemical mechanical grinding for quartz glass. P. Engineering 2010;7:1554–61.
[10] Wang C, Liu Y, Tian J, Niu X, Zheng W, Yue H. Planarization properties of an alkaline slurry without an inhibitor on copper patterned wafer CMP. J. Semicond 2012;33:116001.
[11] Wang LY, Zhang KL, Song ZT, Feng SL. Ceria concentration effect on chemical mechanical polishing of optical glass. Appl Surf Sci 2007;253:4951–4.
[12] Shu Y. Study on etching process of fused silica with concentrated HF. Optik 2019;178:544–9.
[13] Wong L, Suratwala T, Feit MD, Miller PE, Steele R. The effect of HF/NH4F etching on the morphology of surface fractures on fused silica. J Non-Cryst Solids 2009;355:797–810.
[14] Takino H, Yamamura K, Sano Y, Mori Y. Shape correction of optical surfaces using plasma chemical vaporization machining with a hemispherical tip electrode. Appl Optics 2012;51:401–7.
[15] Sun RY, Yang X, Watanabe K, Miyazaki S, Fukano T, Kitada M, Arima K, Kawai K, Yamamura K. Etching Characteristics of Quartz Crystal Wafers Using Argon-Based Atmospheric Pressure CF4 Plasma Stabilized by Ethanol Addition. Nanomanuf Metrol 2019;2:168–76.
[16] Jourdain R, Castelli M, Shore P, Sommer P, Proscia D. Reactive atom plasma (RAP) figuring machine for meter class optical surfaces. Prod. Eng 2013;7:665–73.
[17] Castelli M, Jourdain R, Morantz P, Shore P. Reactive Atom Plasma for Rapid Figure Correction of Optical Surfaces. KEM 2011;496:182–7.
[18] Xin Q, Li N, Wang J, Wang B, Li G, Ding F, Jin H. Surface roughening of ground fused silica processed by atmospheric inductively coupled plasma. Appl Surf Sci 2015;341:142–8.
[19] Yu N, Jourdain R, Gourma M, Shore P. Analysis of De-Laval nozzle designs employed for plasma figuring of surfaces. Int J Adv Manuf Tech 2016;87:735–45.
[20] Yu N, Castelli M, Bennett A, Guo J, Ma CY, Fang FZ. Investigation of a plasma delivery system for optical figuring process. Chinese J Aeronaut CJA 2020;1747:8.
[21] Yi R, Zhang Y, Zhang XQ, Fang FZ, Deng H. A generic approach of polishing metals via isotropic electrochemical etching. Int J Mach Tool Manu 2020;150:103517.
[22] Zhang Y, Chen HYN, Liu DZ, Deng H. High efficient polishing of sliced 4H-SiC (0001) by molten KOH etching. Appl Surf Sci 2020;525:46532.
[23] Ichiki T, Taura R, Horiike Y. Localized and ultrahigh-rate etching of silicon wafers using atmospheric-pressure microplasma jets. J Appl Phys 2004;95:35–9.

[24] Mogab CJ, Adams AC, Flamm DL. Plasma etching of Si and SiO2—The effect of oxygen additions to CF4 plasmas. J Appl Phys 1978;49:3796–803.
[25] Zhang Y, Li RL, Zhang YJ, Liu DZ, Deng H. Indiscriminate revelation of dislocations in single crystal SiC by inductively coupled plasma etching. J Eur Ceram Soc 2019;39:2831–8.
[26] Sarani A, Nikiforov AY, Leys C. Atmospheric pressure plasma jet in Ar and Ar/H2O mixtures: Optical emission spectroscopy and temperature measurements. Phys Plasmas 2010;17:063504.
[27] Song MA, Lee YW, Chung TH. Characterization of an inductively coupled nitrogen-argon plasma by Langmuir probe combined with optical emission spectroscopy. Phys Plasmas 2011;18:023504.
[28] Jung TY, Kim DH, Lim HB. Molecular emission of CF4 gas in low-pressure inductively coupled plasma. B Korean Chem Soc 2006;27:373–6.
[29] Wang R, Zhang C, Liu X, Xie Q, Yan P, Shao T. Microsecond pulse driven Ar/CF4 plasma jet for polymethylmethacrylate surface modification at atmospheric pressure. Appl Surf Sci 2015;328:509–15.
[30] Sano Y, Watanabe M, Kato T, Yamamura K, Mimura H, Yamauchi K. Temperature Dependence of Plasma Chemical Vaporization Machining of Silicon and Silicon Carbide. MSF 2009;600-603:847–50.
[31] Zimmermann S, Ahner N, Blaschta F, Schaller M, Rülke H, Schulz SE, Gessner T. Analysis of the impact of different additives during etch processes of dense and porous low-k with OES and QMS. Microelectron Eng 2010;87:337–42.
[32] Zhu WC, Li Q, Zhu XM, Pu YK. Characteristics of atmospheric pressure plasma jets emerging into ambient air and helium. J Phys D Appl Phys 2009;42:202002.
[33] Zhou RW, Zhang XH, Zong ZC, Li JX, Yang ZB, Liu DP, Yang SZ. Reactive oxygen species in plasma against E. colicells survival rate. Chin. Phys. B 2015;24(08):085201.
[34] Luo Q, Lu J, Xu X, Jiang F. Removal mechanism of sapphire substrates (0001, $112^{-}0$ and $101^{-}0$) in mechanical planarization machining. Ceram Int 2017;43:16178–84.
[35] Castelli M, Jourdain R, Morantz P, Shore P. Rapid optical surface figuring using reactive atom plasma. Precision Engineering 2012;36:467–76.
[36] Laidler KJ. The Development of the Arrhenius Equation. J Chem Educ 1984;61:494–8.